

Ternary Microemulsions as Model Disordered Media

Mark A. Knackstedt and Barry W. Ninham

Dept. of Applied Mathematics, Research School of Physical Sciences and Engineering
The Australian National University, Canberra ACT 0200, Australia

The ternary microemulsion systems alkane/water/DDAB (didodecyltrimethylammonium bromide) form ideal model-disordered media. The static microstructure is described by a simple parameter-free model that can be predetermined and agrees with SAXS and SANS scattering experiments. The component volume fraction can be varied to exhibit bicontinuous random structures with a predicted percolation transition to disconnected water-in-oil droplets. Structural transitions are analyzed in the context of theories of percolative phenomena. Experimental transport properties agree well with model predictions based on an effective medium approximation. Critical exponents that describe the scaling of the transport properties near percolation are consistent with theoretical expectations near a static percolation transition. Through variation of component volume fractions a medium of known microstructure can be prescribed, so that independent measurement of transport and mechanical properties is possible.

Introduction

The determination of effective transport and mechanical properties of disordered media is relevant to a wide variety of phenomena of fundamental and technological interest. A partial list of applications includes flow and dispersion processes in porous media (Sahimi, 1993a), diffusion in catalyst supports and adsorbents (Sahimi et al., 1991), mechanical properties of disordered materials like polymer gels (Stauffer et al., 1982), and conductive and dielectric properties of metal-insulator mixtures (Kirkpatrick, 1973).

One of the simplest prototypes of a disordered medium is the percolation model (Stauffer and Aharony, 1992). The percolation model describes the behavior of a large system, the elements of which are linked in a random manner. In the model, a fraction of the random elements is connected to allow transport. If the number of these elements is small, connection between widely separated points cannot occur, whereas when the number of elements is large the system connectivity is assured and the system becomes macroscopically "percolative." For example, in diffusion studies in catalyst supports a fraction of the pores may be closed to the transport of molecules; pores may be fouled due to the growth or deposition of a solid phase, or, if the diffusing species are

of comparable size to the pores, the pores may be too small to accommodate the diffusing species (Sahimi et al., 1991). The fraction of pores open to molecular transport strongly affects the diffusive properties. The interconnectivity of the elements of a disordered medium and the existence of a sample spanning macroscopic pathway play crucial roles in the overall transport properties of a medium.

While a large body of work exists on theories and simulations to predict geometric and transport properties of disordered media (Sahimi, 1993a), no well-characterized experimental system has been available to test these predictions. Moreover, no system allows the independent measurement of transport and mechanical properties. It is our purpose to describe such a system.

Microemulsions can, under certain conditions, exhibit percolative phenomena (Chen et al., 1984; Ninham et al., 1984; Zemb et al., 1987; Bhattacharya et al., 1985; Kim and Huang, 1986; Moha-Ouchane et al., 1987; Peyrelasse and Boned, 1990; Peyrelasse et al., 1993). For example, upon water dilution water-in-oil microemulsions exhibit changes in electrical conductivity spanning several decades (Chen et al., 1984; Ninham et al., 1984; Zemb et al., 1987; Codastefano et al., 1990, 1992). This behavior is reminiscent of a percolation phenomenon. Several investigations of the ternary

Correspondence concerning this article should be addressed to M. A. Knackstedt.

water/AOT/oil microemulsion (Bhattacharya et al., 1985; Kim and Huang, 1986; Moha-Ouchane et al., 1987; Peyrelasse and Boned, 1990; Peyrelasse et al., 1993) appear to confirm that this system exhibits a *dynamic* percolation behavior (Safran et al., 1985; Grest et al., 1986) characterized by the formation of clusters of interacting water droplets in the continuous oil medium. The characterization of the microstructure of the AOT microemulsions near the transition is problematic; however, the behavior of the AOT/oil/water system is not simply dependent on the volume fraction of the internal phase, but depends as well on an unknown interaction range, on the salt content (Peyrelasse et al., 1993), and on the solubility of AOT in oil. Thus, the variation of transport properties in these systems can only be interpreted *qualitatively* within the framework of percolation theory (Peyrelasse et al., 1993).

Three-component microemulsions formed by double-chain quaternary ammonium surfactants with oil and water (Chen et al., 1984; Ninham et al., 1984; Blum et al., 1985; Fontell et al., 1986; Hyde et al., 1989) have properties that make them ideal model-disordered media. The system most studied comprises didodecyldimethylammonium bromide (DDAB), water, and a C_6-C_{12} alkane. A representative phase diagram of a DDAB/ C_6-C_{12} /water ternary system showing the single-phase microemulsion (L_2) region is given in Figure 1. Throughout most of the region the microemulsion is bicontinuous as inferred from conductivity, diffusivity and small-angle scattering studies. At high water content the microemulsion undergoes a percolative structural transition into water droplets in oil. DDAB is essentially insoluble in both

alkanes and in water, and is therefore constrained to reside at the oil-water interface (Evans et al., 1986). This circumstance allows determination of microstructure relatively easily. An explicit random geometric model, the disordered-open-connected cylinders (DOC) model (Zemb et al., 1987) gives a *parameter-free* interpretation of the microstructure. SAXS and SANS spectra as well as conductivity, viscosity, and diffusivity data are quantitatively consistent with the predicted structure (Barnes et al., 1988).

We analyze the microstructural transition of the DDAB/ C_6-C_{12} /water ternary microemulsion in the context of percolative phenomena. The disordered-open-connected (DOC) model is used to predict the transition from bicontinuous oil/water to disconnected water-in-oil phase. The percolation transition point is in agreement with that deduced from conductivity and diffusivity data. The experimental conductivity and diffusivity measurements near the structural transition point are compared with a theoretical treatment based on the effective medium approximation. The microemulsion exhibits behavior consistent with a static percolation picture. The scaling behavior of the transport and mechanical properties in the vicinity of the microstructural transition are determined. The critical exponents associated with the conductivity, diffusivity, and viscosity of the system are evaluated. The predictions agree with currently accepted values of the exponents for percolation in three dimensions.

Structure and Properties of Water/Alkane/DDAB Microemulsion

The microemulsion phase, L_2 , shown in Figure 1, is a single-phase region within which the DDAB/alkane/water mixture forms a clear, thermodynamically stable isotropic liquid. A feature of this system is that the surfactant has negligible solubility in either alkanes or water. The surfactant therefore resides at and indeed stabilizes the internal interface between the immiscible phase (Evans et al., 1986). This is atypical. For most microemulsions the surfactant may be quite water soluble and may include cosurfactants with high oil and/or water solubilities. DDAB is insoluble in the case of C_6-C_{12} groups forming a lamellar liquid crystal or vesicular dispersion in water (and oil) at concentrations above 10^{-4} molar.

At low-water fractions (see Figure 1) the microemulsions are all electrically conducting; the water phase is continuous (Chen et al., 1984; Ninham et al., 1984). As water is added to the microemulsion, the measured conductivity changes slowly before decreasing abruptly. Over a small range of the ternary phase diagram (along a water dilution line) the conductivity decreases over four decades. NMR studies yield self-diffusion coefficients (Blum et al., 1985; Fontell et al., 1986) that mirror this behavior, the water self-diffusion coefficient decreasing by an order of magnitude or more. Alkane self-diffusion measurements are approximately constant throughout the region. From these observations it is clear that on water dilution there is a percolation-type transition from a structure with connected channels of water permeating the mixture to isolated droplets of water in the continuous oil phase. The alkane remains a continuous phase at all compositions in the L_2 phase.

To experimentally resolve structural details extensive SAXS and SANS studies were undertaken (Barnes et al., 1988).

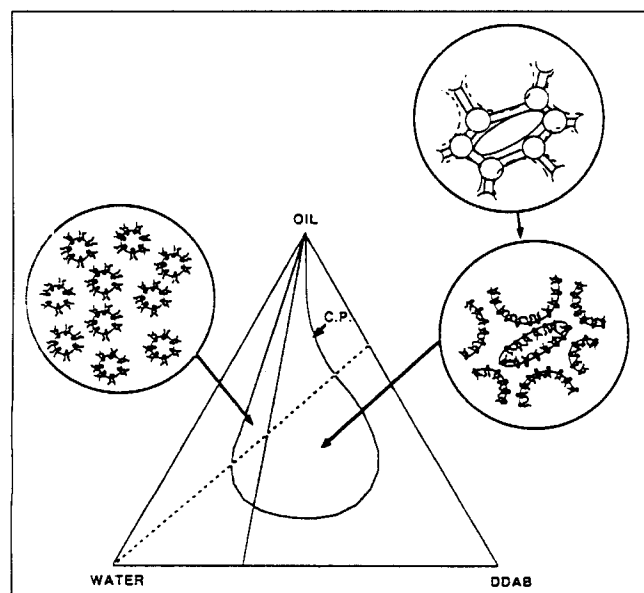


Figure 1. Generic partial phase diagram for a DDAB/alkane/water system.

It shows the L_2 microemulsion region and cross sections of the structures proposed for the different parts of that region. The bicontinuous surface of constant average curvature is approximated in this study by a network of connected spheres and cylinders. The full line ending at the oil corner indicates the percolation threshold line, to the right of which the structure is bicontinuous. The dashed lines indicate typical water dilution paths.

Preexisting models for bicontinuous systems were found to be inadequate to describe—even qualitatively—the DDAB system and the DOC cylinders model (Zemb et al., 1987) was developed to characterize the microemulsion structure. The model predictions are quantitatively consistent with the peak position and the conductivity variation observed in the experimental system. For our later study it is necessary to describe details of this model.

The liquid is divided into randomly distributed oil and water phases. The oil is regarded as a continuous phase in which water with a monolayer of surfactant is dispersed. The microemulsion structure is constrained by the preferred packing configuration of the surfactant molecule in the presence of oil. This shape is characterized by an effective packing parameter (Mitchell and Ninham, 1981) of the surfactant molecule that may include absorbed oil (effective) in the surfactant tails; $(v/al)_{\text{eff}}$. With water alone the surfactant forms a lamellar phase, that is, the surfactant parameter v/al is close to 1.0 where v is the volume of the hydrocarbon tail region, a is the head-group area, and l is an optimal chain length close to the fully extended chain length. With excess water, so that the head groups are fully hydrated, the area a is set primarily by steric constraints and remains essentially constant. With excess oil the tails are swollen by oil penetration (to an amount dependent on the nature of the oil) giving an effective surfactant parameter $(v/al)_{\text{eff}} > 1$. The effective parameter is determined by energetics. It can be inferred from the phase diagram (Hyde et al., 1989).

The DOC model is an analytic approximation to a surface of constant curvature which, to maximize entropy, exhibits no long-range translational order. The topology of the interface is not fixed. The microstructure exhibited by the interface can vary from random monodisperse spheres to highly interconnected structures (cf., Figure 2). The approximation to the actual surface traced out by the surfactant head groups is a network of droplets connected (on average) to Z nearest neighbors by cylindrical segments that satisfy the same curvature constraint. The approximation leads to analytic expressions for the surface area and volume of the internal phase enclosed by the interface. Explicit expressions and details of the model are given in the Appendix. The model yields a unique density of sphere centers n and coordination number Z characterizing the liquid structure for a known water volume fraction and internal surface area (which is directly proportional to the surfactant content).

Prediction of the Microemulsion Structure

The surfactant parameter in the presence of oils is estimated from the high water region of the microemulsion phase (Hyde et al., 1989). The values used in this study are given in Table 1. The packing parameter $(v/al)_{\text{eff}}$ is assumed constant throughout the L_2 phase. Since the oil-swollen volume of the surfactant and extended chain length are fixed, the only possible variable is the area/molecule. SAXS data confirm that this is also constant across the entire microemulsion phase region. We have calculated using the equations given in the Appendix, the variation of the coordination number Z , and density of sphere centers, n , with water content for all the oils listed in Table 1 at various surfactant-to-oil (S/O) ratios. The values for n derived by the model are in agreement with

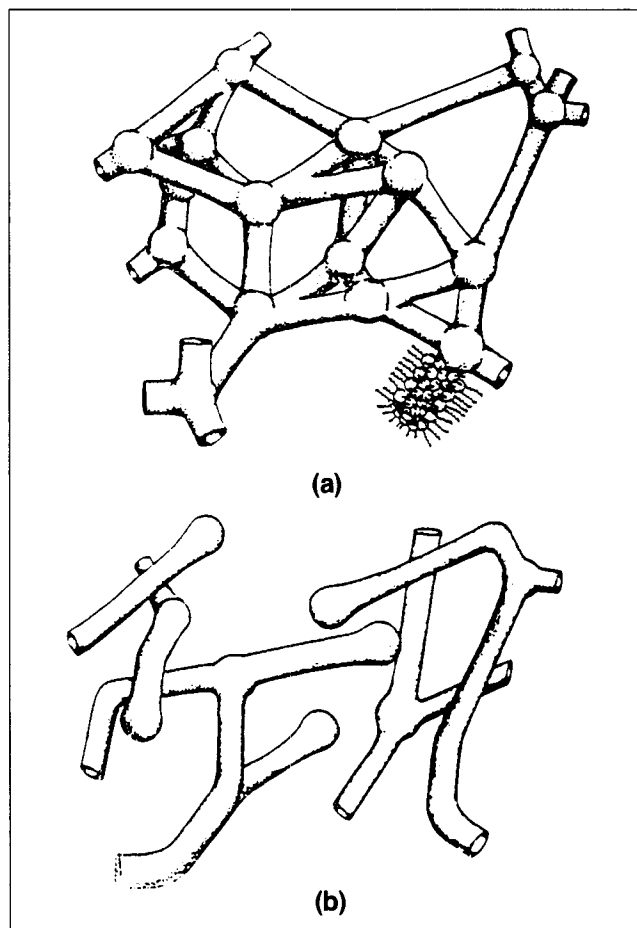


Figure 2. Ternary microemulsion microstructure as described by the DOC model.

(a) 3-D structure with high connectivity, (b) 3-D structure with connectivity below Z_c .

small-angle scattering data. In all cases, the connectivity of the interface varies smoothly throughout the L_2 region, both the geometry and the topology of the surface of constant average curvature varying continuously with water dilution. Figure 3 shows the experimentally measured specific conductance (Chen et al., 1984; Ninham et al., 1984) and the theoretically predicted coordination number as a function of water content for typical sets of experimental data.

Voronoi cells for random hard-sphere packings have an average number of bonds about each vertex of 13.4. In the DOC model an average number Z of these bonds radiating from each vertex is sheathed with cylinders, and are open to trans-

Table 1. Values of the Surfactant Parameter* in the Presence of Different Oils Used in This Study†

Oil	Hexane	Octane	Decane	Dodecane	1-Decene
$\frac{v}{al}$	1.28	1.18	1.15	1.12	1.18

*Hyde et al. (1989).

†These values predict the phase boundaries of the microemulsion.

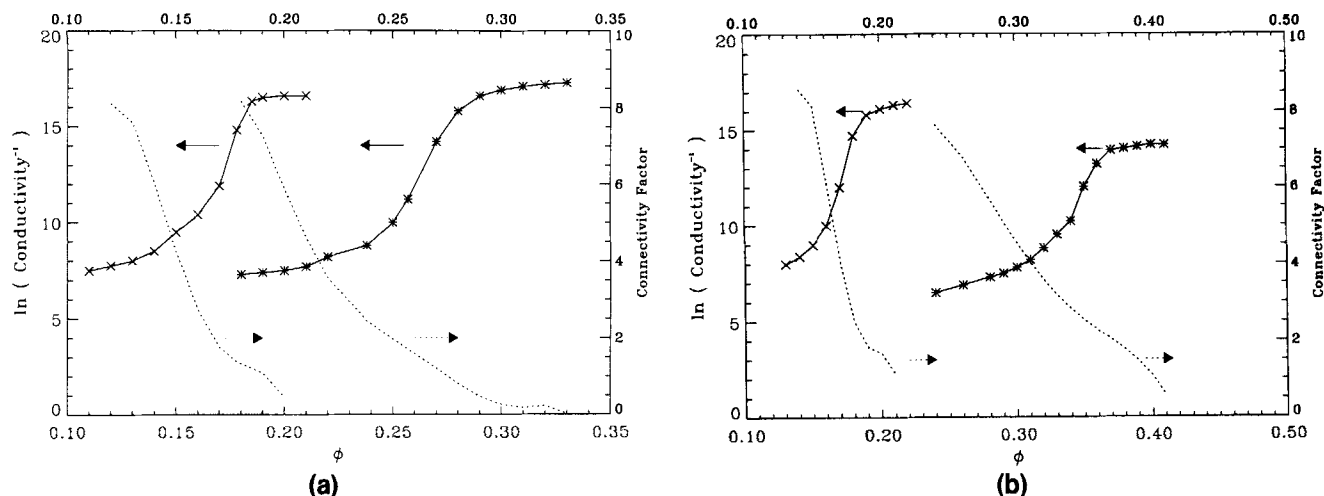


Figure 3. Experimentally measured [Chen et al., 1984; Ninham et al., 1984] conductance data and theoretically predicted coordination number Z as a function of water content.

The solid curve passes through the conductance data. The dashed lines give the average coordination number as predicted by Eqs. 1-3. (a) (\times) Octane ($S/O = 0.176$); (*) decane ($S/O = 0.250$). (b) (\times) 1-Hexene ($S/O = 0.250$); (*) 1-hexene ($S/O = 0.667$).

port/conduction. If Z is large, the network is well-connected. At some well-defined value of Z defined as Z_c , the percolation threshold, there is a transition in the topological structure of the random network from a well-connected structure to a disconnected one. The normalized bond percolation threshold for the so-called VOR14 network (Jerauld et al., 1984), the Voronoi tessellation with average coordination of 14, is $p_c = 0.0956$. We approximate the percolation threshold of the DOC network by $Z_c = 13.4p_c \approx 1.3$.

Consider the observed conductivity variation as a percolation transition. The DOC model predicts that the coordination of the three-dimensional (3D) random networks decreases upon water dilution (see Table 2 and Figure 3). The initial decrease in coordination leads to a slow drop in the conductivity, followed by an abrupt decrease in the conductivity at high water content due to the loss of continuous paths through the water region of the microemulsion. The model prediction for the conducting/nonconducting transition point ($Z \approx 1.3$) is in excellent agreement with the experimentally observed transition from a conducting to a nonconducting medium (cf. Figure 3 and Table 2). In particular, Figure 3b illustrates how well the DOC model describes the microemulsion structure across the microemulsion phase region. In this case, despite the widely differing S/O ratio in the two 1-hexene systems, the transition point is given accurately in both cases.

A careful study of NMR self-diffusion has been carried out on the ternary microemulsion DDAB/dodecane/water at various S/O ratios (Blum et al., 1985; Fontell et al., 1986). Results of these studies mirror the conductivity studies—the water self-diffusion coefficients are found to be highly concentration dependent and to exhibit regions where water molecules are confined to small domains, the water self-diffusion constant varying by up to two orders of magnitude upon dilution. We have calculated the variation of the coordination number Z with water content for three (S/O) ratios. The results are summarized in Table 3 and in Figure 4. From the prediction for Z given by the random geometric model, in

two of the three cases ($S/O = 0.333$ and ($S/O = 0.441$ the water dilution is not sufficient to reach the microstructural threshold ($Z_c \approx 1.3$). The experimental data mirror this behavior (cf. Table 3). The self-diffusion constant is reduced from the low water-dilution value, but remains larger than the self-diffusion constant expected if no connected water pathway were present. For the third system ($S/O = 0.184$), the model predicts that the transition does occur within the experimental bounds (at $\phi_{\text{water}} \approx 0.60$). This result is mirrored in the data. The water self-diffusion coefficient is over two orders of magnitude smaller than the value in the water continuous regime ($Z > 1.3$).

Viscosity data for octane and decane microemulsions was obtained along water dilution lines in the L_2 region (Chen et

Table 2. Experimental Quantities* and Model Prediction for the System DDAB/Octane/Water with a Surfactant-to-Oil Ratio (S/O) = 0.176 and an Effective Surfactant Parameter $(v/al)_{\text{eff}} = 1.18^\dagger$

ϕ_{water}	ϕ_{int}	$\Sigma(\text{\AA}^{-1})$	$-\log(\sigma)$ (ohm $^{-1} \cdot \text{cm}^{-1}$)	$r_s(\text{\AA})$	Z
0.11	0.098	0.00875	7.5	40	8.2
0.12	0.106	0.00867	7.75	44	8.1
0.13	0.113	0.00860	8.0	46	7.5
0.14	0.121	0.00853	8.5	49	6.45
0.15	0.129	0.00845	9.0	50	3.7
0.16	0.137	0.00837	10.4	52	2.9
0.17	0.145	0.00830	12.2	54	1.9
0.178	0.152	0.00823	14.8	57	1.4
0.185	0.157	0.00818	16.3	58	1.1
0.19	0.161	0.00814	16.5	60	1.05
0.20	0.169	0.00806	16.6	63	0.5
0.21	0.177	0.00798	16.6	67	0.25

*Chen et al. (1984).

† Compositions and measured quantities for the sample are given in columns 1-4. Columns 5 and 6 give the parameters resulting from a fit to the DOC model, where r_s is the sphere radius and Z the coordination number.

Table 3. Experimental Quantities* and Model Prediction for the System DDAB/Octane/Water[†]

$(S/O)_{\text{molar}}$	ϕ_{DDAB}	ϕ_{dodecane}	ϕ_{water}	D_w ($10^{-10} \text{ m}^2 \cdot \text{s}^{-1}$)	r_s (Å)	Z
0.184	0.261	0.543	0.196	3.63	35	8.3
	0.250	0.499	0.251	3.11	37	8.0
	0.210	0.440	0.350	1.01	66	6.7
	0.180	0.370	0.450	0.18	87	3.45
	0.160	0.340	0.500	0.10	107	2.4
	0.130	0.270	0.600	0.02	159	1.05
0.333	0.379	0.420	0.201	3.65	27	10.0
	0.342	0.391	0.267	3.51	34	8.6
	0.303	0.347	0.350	2.70	46	7.6
	0.269	0.307	0.423	2.04	58	7.1
	0.249	0.273	0.478	1.21	67	4.8
	0.210	0.240	0.550	0.31	89	3.55
0.441	0.401	0.351	0.248	3.95	29	9.4
	0.386	0.338	0.276	3.56	32	8.9
	0.327	0.286	0.387	3.16	39	9.2
	0.302	0.257	0.441	2.89	54	7.0
	0.284	0.242	0.474	1.13	58	5.5
	0.252	0.224	0.524	1.09	71	4.4
	0.229	0.195	0.576	0.33	82	3.5

*Fontell et al., 1986.

[†]Surfactant-to-oil ratios are given in molar concentrations, and ϕ denotes composition by weight. The effective surfactant parameter used is $(v/a)_{\text{eff}} = 1.12$ (Hyde et al., 1989). Compositions and measured quantities for the sample are given in columns 1–5. Columns 6 and 7 give the parameters resulting from a fit to the DOC model, where r_s is the sphere radius and Z the coordination number.

al., 1984). The microemulsions exhibit a high viscosity in the bicontinuous low-water content region, which decreases steadily as water is added. The minimum in the viscosity curve coincides with the conductivity transition (Chen and Warr, 1992). We have calculated the variation of the coordination number Z as a function of water content. The results are

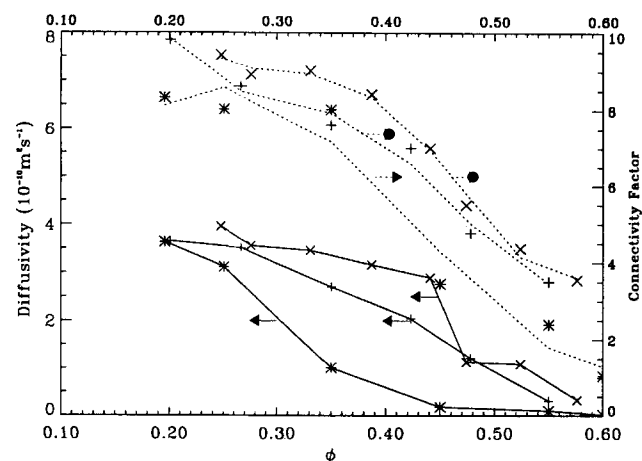


Figure 4. Experimentally measured (Fontell et al., 1986) diffusivity data and theoretically predicted coordination number Z as a function of water content.

(*) Dodecane ($S/O = 0.185$); (+) dodecane ($S/O = 0.333$); (x) dodecane ($S/O = 0.441$). The solid curve passes through the conductance data; the dashed lines give the average coordination number as predicted by Eqs. 7–9.

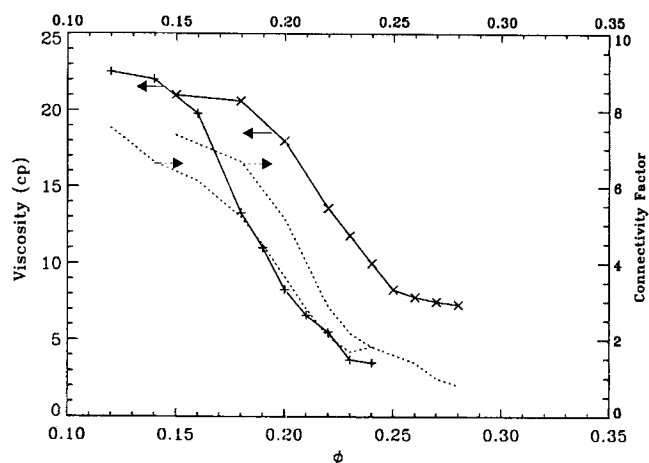


Figure 5. Experimentally measured (Chen et al., 1984) viscosity data and theoretically predicted coordination number Z as a function of water content.

(+) Octane ($S/O = 0.293$); (x) decane ($S/O = 0.250$). The solid curve passes through the experimental data; the dashed line gives the average coordination number as predicted by Eqs. 7–9.

summarized in Figure 5 and in Table 4. A general trend of reduced viscosity as the coordination number decreases is evident.

The prediction of the structural transition point of the microemulsion illustrates the efficacy of this simple parameter-free interpretation of the microstructure based on physical concepts such as mass action rules, surface interactions, and geometrical packing constraints. Since the microstructure of the DDAB/ C_6 – C_{12} /water system can be well-characterized

Table 4. Experimental Quantities* and Model Prediction for the Systems DDAB/Octane/Water with $(S/O) = 0.293$ and DDAB/Decane/Water with $(S/O) = 0.250$ [†]

Oil	ϕ_{water}	η_{measured} (cp)	Z
Octane	0.12	22.5	9.44
	0.14	22.0	8.3
	0.16	19.8	7.5
	0.18	13.3	6.7
	0.19	11.0	6.0
	0.20	8.3	4.0
	0.21	6.6	3.25
	0.22	5.5	2.8
	0.23	3.7	2.4
Decane	0.15	21.0	9.3
	0.18	20.6	9.2
	0.20	18.0	6.5
	0.22	13.6	3.5
	0.23	11.8	2.65
	0.24	10.0	2.45
	0.25	8.3	1.95
	0.26	7.8	1.6
	0.27	7.5	1.3

*Chen et al., 1994.

[†]Compositions and measured quantities for the sample are given in columns 1 and 2. Column 3 gives the coordination number Z resulting from a fit to the DOC model.

theoretically and because the microemulsion exhibits a percolation threshold, we expect the ternary DDAB microemulsion to be an ideal experimental model-disordered media. In the next section model predictions of the electrical and diffusive properties of the microemulsions are compared with experiment.

Effective-Medium Approximation

One of the simplest methods of estimating the effective transport properties of disordered media is the effective-medium approximation (EMA). This is a phenomenological method by which a disordered medium is replaced with a hypothetical homogeneous one with unknown physical constants. In the original EMA developed by Bruggeman (1935), each inhomogeneity is embedded in the effective medium itself, the unknown properties of which are determined so that the volume average over all inhomogeneities yields no extra field in the medium. Kirkpatrick (1973) extended the Bruggeman method to the study of random networks. He showed that for a network of coordination number Z , the EMA predicts that

$$f(g) \frac{g - \sigma_e}{g + A\sigma_e} dg = 0 \quad (1)$$

where $A = (Z/2) - 1$ and $f(g)$ is the pore conductance distribution. For our system $f(g)$ is given by

$$f(g) = p_o \delta(g - g_o) + p_i \delta(g - g_i) \quad (2)$$

where p_i is the fraction of bonds in the internal phase defined by $Z/13.4$; Z is given by the solution to the DOC model; and $p_o = 1 - p_i$. The brine conductivity g_i and the oil conductivity g_o are taken to be the asymptotic values (Figure 3) of the conductivities of the microemulsion at $Z = Z_{\max}$ and $Z = 0.0$, respectively. We show in Figure 6, the prediction of the effective-medium theory and compare with the experimental data across the full range of the conductivity measurements. The agreement is good in all cases. In particular, given the large variation in the S/O ratio in the 1-decene system (Figure 6c), the agreement is satisfying.

The effective-medium theory for resistor networks can also be used to find the effective diffusivity of a random medium (Davis, 1977). Using Eqs. 1 and 2 and replacing g_i by the asymptotic diffusivity measured at high coordination number and setting $g_o = 0$ enables us to make a prediction of the effective water self-diffusivity D_w in the microemulsion phase. The prediction of the EMA and the comparison with experiment is given in Figure 7. The quantitative prediction of the transport (conductive and diffusive) properties near the microstructural transition is a further indication of the efficacy of the DOC model in describing microstructure exhibited by ternary microemulsions.

We note that the EMA used earlier is expected to only give *qualitatively* reasonable results. In the preceding approximation we assume that the effective conductance of each pore presents the same overall resistance to diffusion/conduction at all water contents. This is clearly an approximation. The sphere and cylinder radii vary across the region as

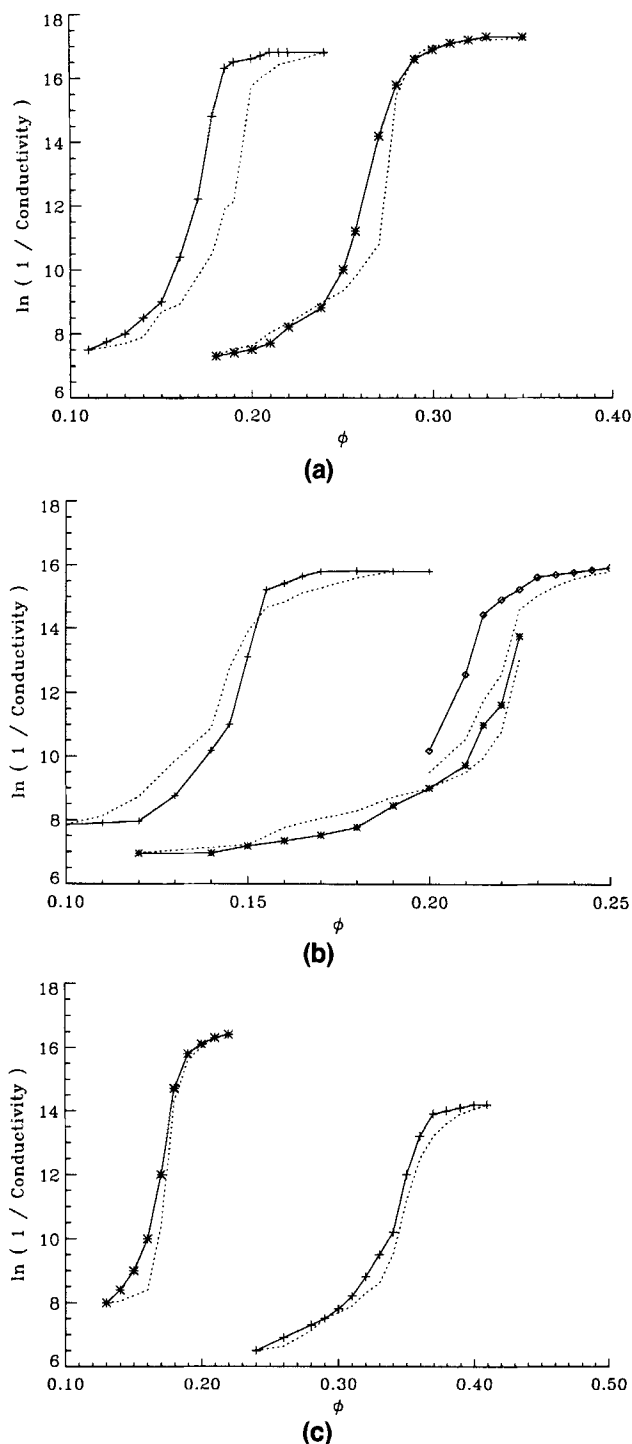


Figure 6. Experimental conductance data (—) vs. EMA prediction (---).

(a) (+) Octane and (*) decane. (b) (+) Hexane ($S/O = 0.253$); (\diamond) hexane ($S/O = 0.389$); (*) hexane ($S/O = 0.412$). (c) (*) 1-Hexene ($S/O = 0.250$); (+) 1-hexene ($S/O = 0.667$).

predicted by the random geometric model (see Tables 2 and 3). This variance in the sphere size should be accounted for in the study of transport properties (Burganos and Sotirchos, 1987). It should also be noted that the EMA is expected to

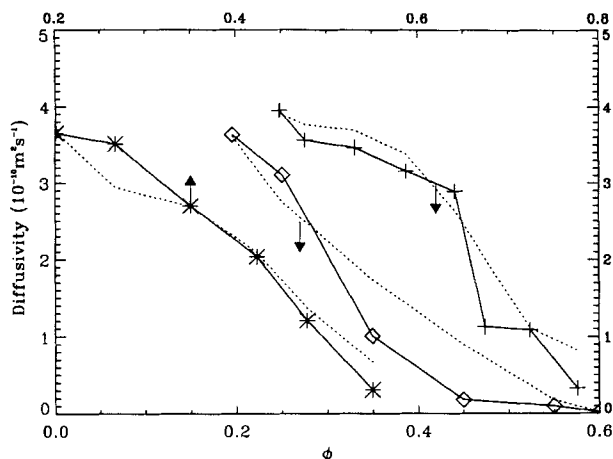


Figure 7. Experimental water self-diffusion constant data (—) vs. EMA prediction (---).

(◇) Dodecane ($S/O = 0.185$); (*) dodecane ($S/O = 0.333$); (+) dodecane ($S/O = 0.441$).

be accurate everywhere but near a percolation threshold. More refined theories of transport near percolative transitions can be utilized. For example, the renormalized effective-medium approach (REMA) has enjoyed much success (Sahimi et al., 1983). The exact solution to the conductivity problem on the Bethe network of coordination number Z has also been used as an accurate approximation to the conductivity of 3-D networks (Stinchcombe, 1974; Sahimi, 1993b). These methods can be used to compare the theoretical prediction with the experimental data, yielding more accurate predictions of transport properties than a simple EMA. The analysis of a more comprehensive experimental study near p_c will warrant the use of these more accurate approximations.

Scaling of the Transport Properties Near the Percolation Threshold

Of particular interest in the study of transport in and me-

chanical properties of disordered media, is the behavior of the properties in the vicinity of the percolation threshold (Stauffer and Aharony, 1992). For example, the behavior of the effective conductivity of the percolative medium near p_c ($= Z_c/13.4$) is described (for $p > p_c$) by

$$\sigma_e = (p - p_c)^{\mu_E} \quad (3)$$

where μ_E is a critical exponent. It is believed that the exponent μ_E is universal and depends only on the dimensionality of the medium. This hypothesis is supported by numerous theoretical studies and numerical calculations. The currently accepted value of the conductivity exponent is $\mu_E \approx 2.0$ (Stauffer and Aharony, 1992). From the coordination number Z given by the DOC model and the experimental conductivity data, we can evaluate μ_E for the microemulsion. The plots of $\ln(1/\sigma)$ vs. $\ln(p - p_c)$ are shown in Figure 8a for the octane and decane systems, in Figure 8b for the hexane systems, and in Figure 8c for the 1-decene system. The value of the critical exponents derived from the data are given in Table 5. The experimental data are in agreement with the currently accepted values for static percolation; $\mu_E \approx 2.0$.

The behavior of the effective diffusivity D_e of the microemulsion near p_c is also of particular interest. Since D_e is proportional to σ_e ,

$$\sigma_e = (\phi D_e) \quad (4)$$

where ϕ denotes the media porosity, D_e has the same power law dependence on p near p_c as that of σ_e . The evaluation of the exponent associated with the diffusivity μ_D is shown in Figure 9. The value of μ_D is consistent with the value of μ_E .

The power law dependence of D_e on p is valid only if the linear size of the system is larger than the correlation length ξ of the medium, and if a long enough time has elapsed (Sahimi et al., 1991). In the self-diffusion experiments the time between the first 90° pulse and the echo pulse was kept constant at 140 ms. This time is long enough to ensure that the water (even at the lowest measured D_w) travels a distance of

Table 5. Conductivity and Diffusivity Exponents Derived from the Experimental Data*†

A. Conductivity				
Oil	Hexane	Octane	Decane	1-Decene
μ_E	$1.6 \pm 0.3 \left(\frac{S}{O} = 0.253 \right)$ $1.6 \pm 0.5 \left(\frac{S}{O} = 0.441 \right)$	$1.8 \pm 0.2 \left(\frac{S}{O} = 0.176 \right)$	$1.8 \pm 0.2 \left(\frac{S}{O} = 0.250 \right)$	$2.3 \pm 0.2 \left(\frac{S}{O} = 0.250 \right)$ $2.2 \pm 0.2 \left(\frac{S}{O} = 0.667 \right)$
B. Diffusivity				
Oil	Dodecane			
μ_D	$1.4 \pm 0.4 \left(\frac{S}{O} = 0.185 \right)$ $1.85 \pm 0.4 \left(\frac{S}{O} = 0.333 \right)$ $1.85 \pm 0.4 \left(\frac{S}{O} = 0.441 \right)$			

*Chen et al. (1984); Fontell et al. (1986).

†The theoretical prediction for the conductivity and diffusivity exponent is $\mu_E = \mu_D \approx 2.0$.

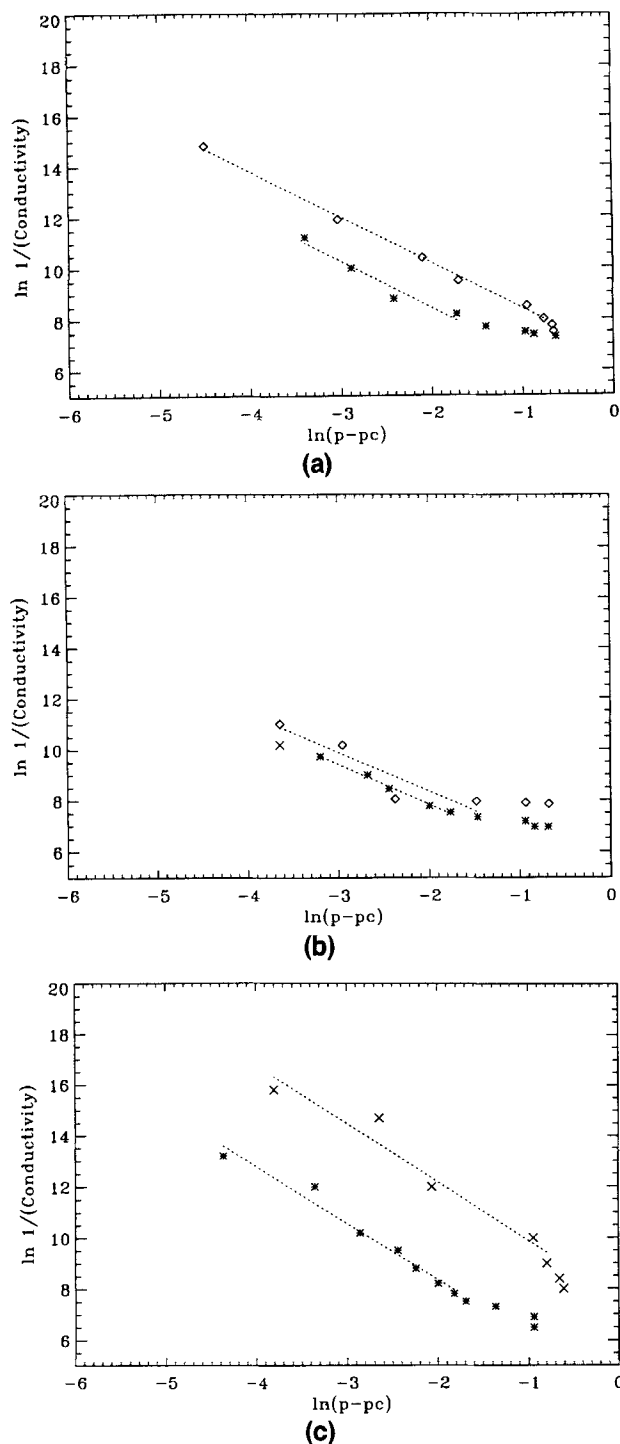


Figure 8. Evaluation of the conductivity exponent μ_E for the microemulsion.

(a) (*) Decane and (◇) octane. Slopes of the linear least-squares fit are 1.82 and 1.79, respectively. (b) (*) Hexane ($S/O = 0.253$); (◇) hexane ($S/O = 0.412$). Slopes of the linear least-squares fit are 1.59 and 1.63, respectively. (c) (×) 1-Hexene ($S/O = 0.250$); (*) 1-hexene ($S/O = 0.667$). Slopes of the linear least-squares fit are 2.29 and 2.21, respectively.

about a micron. For media away from critical ($Z > 2.0$) this length scale is greater than any structural correlation. To obtain the short time behavior of D_e , or the behavior of D_e for

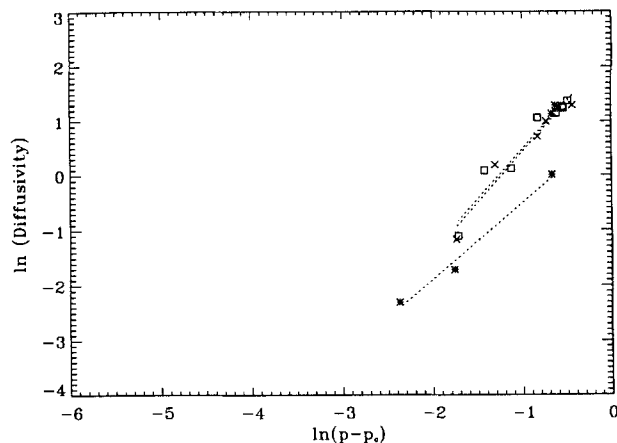


Figure 9. Evaluation of the diffusivity exponent μ_D for the microemulsion.

(*) Dodecane ($S/O = 0.185$); (×) dodecane ($S/O = 0.333$); (◇) dodecane ($S/O = 0.441$). Slopes of the linear least-squares fit are 1.41, 1.85 and 1.85, respectively.

systems with linear size L less than ξ , is of interest (Sahimi et al., 1991). In a d -dimensional system, the mean-squared displacement of the particles, $\langle x^2(t) \rangle$ is related to the effective diffusivity and time t as

$$\langle x^2(t) \rangle = 2dD_e t. \quad (5)$$

If D_e is constant, then $\langle x^2(t) \rangle$ grows linearly with t , and one obtains the usual Fick law between the flux, concentration gradient, and D_e . However, this would be true only if $\langle x(t) \rangle = [\langle x^2(t) \rangle]^{1/2}$ is much larger than the length scale over which the disordered medium is homogeneous. This length scale for a percolation system is the correlation length ξ , which diverges at p_c . Thus, if a finite system is near its percolation threshold (for example, a catalyst particle nearing complete deactivation) one may not have normal diffusion with $\langle x^2(t) \rangle$ growing linearly in time, but rather $\langle x^2(t) \rangle \sim t^\alpha$ where $\alpha < 1$. Thus, D_e depends on time and vanishes as $t \rightarrow \infty$. The ternary DDAB/alkane/water microemulsion near the microstructural transition point is an ideal system for the experimental study of anomalous diffusive behavior.

There is interest in the rheological behavior of chemical gels near the sol-gel transition (Stauffer et al., 1982). A gelling solution at the sol-gel transition has unique properties. The viscosity of the solution is infinite, whereas the elastic modulus is zero. Across the transition the system transforms from a viscous liquid medium to an elastic medium. The transition is modeled as a percolative transition. For $p < p_c$ one has a sol, which is a viscous assembly of polydisperse finite clusters, and for $p > p_c$, there is a sol embedded in an "infinite" gel (a connected cluster that spans the system).

Experimental measurements indicate that near the gel transition, the viscosity η diverges with an exponent k ($\eta \sim (p - p_c)^{-k}$). The value of k can be either in the range 1.3–1.5 (Martin et al., 1988) or 0.6–0.8 (Adam et al., 1981, 1985), depending on experimental conditions. A superelastic percolation model (Arbabi and Sahimi, 1990) was proposed to explain the different observed behaviors. In the model two limiting cases were studied. The first case (Zimm limit) assumes

strong hydrodynamic interaction between clusters (diffusion of clusters is hindered and there is no significant cluster movement), and the second case (Rouse limit) assumes no hydrodynamic interactions (clusters are free to diffuse through the system). In the first case the behavior of the system can be described by a static percolation network, and the exponent k describing the viscosity divergence is $k \approx 0.65$. In the latter case the exponent is $k \approx 1.30$. The exponent k describing the divergence of the octane and decane microemulsion viscosity near the threshold ($Z_c \approx 1.3$) is given by (see Figure 10) $k \approx 0.40 (\pm 0.2)$ and $k \approx 0.75 (\pm 0.2)$. In the DDAB system the surfactant is insoluble in either phase. We anticipate that the system is stable to rearrangement and can be modeled as a static percolative system. The exponent k for the system is in good agreement with predictions near a sol-gel transition in the Zimm limit.

It should be noted that the rheological properties of a sol-gel transition in the Zimm limit are very different from the DDAB microemulsion. In the gel transition the viscosity *diverges* as the percolation threshold is approached from *below* [$\eta \sim (p - p_c)^{-k}$ for $p < p_c$]. In our system k describes the *increase* in the viscosity *above* the transition ($\eta \sim (p - p_c)^k$ for $p > p_c$). The percolation model (Arbabi and Sahimi, 1990) developed to explain the viscosity divergence proposes that the behavior of η near p_c is similar to that of the shear modulus of an elastic percolation network below p_c where the fraction $p < p_c$ of bonds are *superelastic*—they exhibit an infinite local stretching/bending constant. In contrast, the DDAB system is analogous to an elastic percolative network with a fraction $p > p_c$ of bonds exhibiting a *finite* bending/stretching constant and the rest of the bonds ($1 - p$) exhibiting no elastic constant. Simulations of critical elastic properties of systems in this regime yield an exponent in the range 3.5–3.8. It is not yet clear how to interpret the scaling behavior of the viscosity of the DDAB system.

Discussion

The microstructure of the ternary system formed from

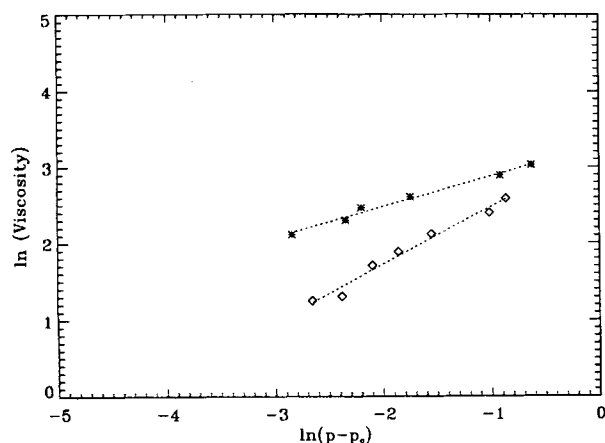


Figure 10. Evaluation of the viscosity exponent k for the microemulsion.

(*) Octane ($S/O = 0.293$); (×) decane ($S/O = 0.250$). Slopes of the linear least-squares fit are 0.40 and 0.75, respectively.

double-chained cationic amphiphiles, water, and alkanes or alkenes can be understood in terms of *elementary* concepts that derive from and link directly to theories of surfactant/water aggregation. The surfactants are virtually insoluble in both water and oil and are therefore constrained to reside at the oil-water interface. This makes the unravelling of the microstructure relatively easy. The DOC model, utilizing principles that govern self-assembly, allows the microstructure of these microemulsions to be identified and well-characterized. In this article we have discussed the microstructural transition of the ternary DDAB/alkane/water microemulsion in the context of percolative phenomena. The simple, parameter-free (DOC) interpretation of the microstructure is found to predict the percolative transition point accurately. Comparison of the experimentally measured transport properties with a theoretical treatment based on the simple effective medium treatment is satisfactory. Evaluation of the critical exponents describing the scaling of the transport properties near a percolation threshold are consistent with properties exhibited near a static percolative transition.

Ternary microemulsions have previously been studied as model percolative media. In particular, the AOT/water/decane system has been considered a useful system for studying electrical conductivity and viscous percolative phenomena (Bhattacharya et al., 1985; Kim and Huang, 1986; Moha-Ouchane et al., 1987; Peyrelasse and Boned, 1990; Codastefano et al., 1990, 1992; Peyrelasse et al., 1993). The microemulsion incorporating AOT as the surfactant, however, differs quite markedly from the system incorporating DDAB. First, throughout most of the L_2 phase the AOT/water/decane system forms a water-in-oil microemulsion. Upon water dilution the system exhibits a rapid increase in electrical conductivity. Investigations confirm that this is a *dynamic* percolation phenomenon (Safran et al., 1985; Grest et al., 1986), characterized by the formation of a cluster of water droplets within a continuous oil medium. Experimental (Bug et al., 1986; Peyrelasse et al., 1993) and theoretical (Grest et al., 1986; Seaton and Glandt, 1987) studies have shown that the attractive interactions between the isolated globules of water-in-oil are crucial to understanding the observed increase in the conductivity. The picture that has emerged for the transition involves the formation of clusters of water globules that are sufficiently close to each other that an effective transfer of charge carriers can take place. This accounts for the experimental observation that the microemulsion exhibits percolative behavior at anomalously small volume fractions. Percolative phenomena in systems of interacting objects are complicated. In such systems it is not only the density ϕ of the dispersed phase that governs the existence of percolation, but also the interactions between objects that cause correlations of positions. A current theoretical problem concerns the prediction of the relationship between the percolation threshold and the interaction strength (Xu and Stell, 1989).

Variation of conductivity, dielectric relaxation, and viscosity in AOT/water/decane systems can only be interpreted *qualitatively* within the framework of ordinary percolation theory. The behavior of the AOT system does not simply depend on the magnitude of $(\phi - \phi_c)$, where ϕ_c is the volume fraction of the internal phase at the conductivity transition point, but depends as well on the unknown interaction range,

on salt content (Peyrelasse and Boned, 1990), and on the solubility of oil in AOT. Quantitative determination of the percolation threshold and properties requires the development of a theory able to predict the extent of the interglobule interactions and of experimental understanding of the range and strength of the interparticle force (Peyrelasse et al., 1993).

By contrast, the DDAB/ C_6-C_{12} /water system exhibits a wide range of microstructure that, most importantly, can be predicted from elementary concepts. In the DDAB system the surfactant can be assumed to reside solely at, and indeed to stabilize the internal interface between, the immiscible phases. In the AOT system where the surfactant is soluble in the water the microemulsion must be considered as a fluctuating entity. In the DDAB system we anticipate that the Z coordinated water channels are stable to rearrangement. The system allows one to tune experimental variables to give a specific microstructure and moreover, allows the determination of various transport and mechanical properties; the conductivity, diffusivity, and viscosity (Chen and Warr, 1992) can be independently measured. The ternary DDAB/ C_6-C_{12} /water systems is a most appropriate candidate for the experimental study of transport properties in 3-D percolative media. A more comprehensive study of the effect of morphology on transport properties in DDAB/alkane/water microemulsions and an experimental study of anomalous diffusion properties exhibited near the percolation transition is planned. Finally, ternary microemulsion systems monomer/water/DDAB have been shown to exhibit a predictable microstructure. The mixture has been polymerized to produce a solid porous material with a well-defined microstructure (Ninham et al., 1992). This enables one to study flow, dispersion, and displacement processes in well-defined disordered media.

NMR self-diffusion measurements in ternary DDAB microemulsions near the structural transition point have recently been performed. Time-dependent diffusion is experimentally observed. Details of the experiment are to be published elsewhere (Knackstedt et al., 1995).

Acknowledgment

One of the authors (M.A.K.) would like to thank the Rothmans Foundation of Australia and the Australian Research Council for support.

Notation

D	= Euclidean dimension
f	= conductance distribution
g	= conductance
L	= network size
p_o	= fraction of bonds in external phase
x	= distance
Z_{\max}	= maximum value of coordination number

Greek letters

α	= exponent of anomalous diffusion
ϕ	= volume fraction of internal phase

Literature Cited

- Adam, M., M. Delsanti, D. Durand, G. Hild, and J. P. Munch, "Mechanical Threshold Near Gelation Threshold, Comparison with Classical and 3D Percolation Theories," *Pure Appl. Chem.*, **53**, 1489 (1981).
- Adam, M., M. Delsanti, and D. Durand, "Mechanical Measurements in the Reaction Bath During the Polycondensation Reaction Near the Gelation Threshold," *Macromol.*, **18**, 2285 (1985).
- Arbabi, S., and M. Sahimi, "Critical Properties of Viscoelasticity of Gels and Elastic Percolation Networks," *Phys. Rev. Lett.*, **65**, 725 (1990).
- Barnes, I. S., S. T. Hyde, B. W. Ninham, P.-J. Derian, M. Drifford, and T. N. Zemb, "Small-Angle X-Ray Scattering from Ternary Microemulsions Determines Microstructure," *J. Phys. Chem.*, **92**, 2286 (1988).
- Bhattacharya, S., J. P. Stokes, M. W. Kim, and J. S. Huang, "Percolation in Oil Continuous Microemulsions," *Phys. Rev. Lett.*, **55**, 1884 (1985).
- Blum, F. D., S. Pickup, B. W. Ninham, S. J. Chen, and D. F. Evans, "Structure and Dynamics in Three-Component Microemulsions," *J. Phys. Chem.*, **89**, 711 (1985).
- Bruggeman, D. A. G., "Berechnung verschiedener physikalischer konstanten von heterogenen substanzen: I. dielectrizitätskonstanten und leitfähigkeiten der mischkörper aus isotropen substanzen," *Ann. Phys.*, **24**, 636 (1935).
- Bug, A. L. R., S. A. Safran, G. S. Grest, and I. Webman, "Dynamic Percolation in Microemulsions," *Phys. Rev. Lett.*, **55**, 1896 (1986).
- Burganos, V. N., and S. V. Sotirchos, "Diffusion in Pore Networks: Effective Medium Theory and Smooth Field Approximation," *AIChE J.*, **33**, 1678 (1987).
- Chen, C.-M., and G. G. Warr, "Rheology of Ternary Microemulsions," *J. Phys. Chem.*, **96**, 9492 (1992).
- Chen, S. J., D. F. Evans, and B. W. Ninham, "Properties and Structure of Three-Component Microemulsions," *J. Phys. Chem.*, **88**, 1631 (1984).
- Codastefano, P., C. Cametti, P. Tartaglia, S. H. Chen, and J. Rouch, "Theory and Experiment of Electrical Conductivity and Percolation Locus in Water-in-Oil Microemulsions," *Phys. Rev. Lett.*, **64**, 1461 (1990).
- Codastefano, P., C. Cametti, P. Tartaglia, S. H. Chen, and J. Rouch, "Electrical Conductivity and Percolation Phenomena in Water-in-Oil Microemulsions," *Phys. Rev. A*, **45**, 5358 (1992).
- Davis, H. T., "The Effective Medium Theory of Diffusion in Composite Media," *J. Amer. Ceram. Soc.*, **60**, 499 (1977).
- Evans, D. F., D. J. Mitchell, and B. W. Ninham, "Oil Water and Surfactant: Properties and Conjectured Structure of Simple Microemulsions," *J. Phys. Chem.*, **90**, 2817 (1986).
- Fontell, K., A. Ceglie, B. Lindman, and B. W. Ninham, "Some Observations on Phase Diagrams and Structure in Binary and Ternary Systems of Didodecyldimethylammonium Bromide," *Acta Chem. Scand. A*, **40**, 247 (1986).
- Grest, G. S., I. Webman, S. A. Safran, and A. L. R. Bug, "Dynamic Percolation in Microemulsions," *Phys. Rev. A*, **33**, 2842 (1986).
- Hyde, S. T., B. W. Ninham, and T. N. Zemb, "Phase Boundaries for Ternary Microemulsions. Predictions of a Geometric Model," *J. Phys. Chem.*, **93**, 1464 (1989).
- Jerauld, G. R., L. E. Scriven, and H. T. Davis, "Percolation and Conduction on the 3D Voronoi and Regular Networks: A Second Case Study in Topological Order," *J. Phys. C*, **17**, 3429 (1984).
- Kim, M. W., and J. S. Huang, "Percolation-Like Phenomena in Oil Continuous Microemulsions," *Phys. Rev. A*, **34**, 719 (1986).
- Kirkpatrick, S., "Percolation and Conduction," *Rev. Mod. Phys.*, **45**, 573 (1973).
- Knackstedt, M. A., M. Monduzzi, and B. W. Ninham, "Diffusion in Model Disordered Media," *Phys. Rev. Lett.*, submitted (1995).
- Martin, J. E., D. Adolff, and J. P. Wilcoxon, "Viscoelasticity of Near-Critical Gels," *Phys. Rev. Lett.*, **61**, 2620 (1988).
- Mitchell, D. J., and B. W. Ninham, "Micelles, Vesicles and Microemulsions," *J. Chem. Soc. Farad. Trans. 2*, **77**, 601 (1981).
- Moha-Ouchane, M., J. Peyrelasse, and C. Boned, "Percolation Transition in Microemulsions: Effect of the Water-Surfactant Ratio, Temperature and Salinity," *Phys. Rev. A*, **35**, 3027 (1987).
- Ninham, B. W., S. J. Chen, and D. F. Evans, "Role of Oils in Microemulsion Design," *J. Phys. Chem.*, **88**, 5855 (1984).
- Ninham, B. W., S. T. Hyde, and R. Pashley, "Formation of Porous Materials," U.S. patent pending (1992).
- Peyrelasse, J., and C. Boned, "Conductivity, Dielectric Relaxation, and Viscosity of Ternary Microemulsions: The Role of the Experi-

- mental Path and the Point of View of Percolation Theory," *Phys. Rev. A*, **41**(2), 938 (1990).
- Peyrelasse, J., C. Boned, and Z. Saidi, "Quantitative Determination of the Percolation Threshold in Waterless Microemulsions," *Phys. Rev. A*, **47**, 3412 (1993).
- Safran, S. A., I. Webman, and G. S. Grest, "Percolation in Interacting Colloids," *Phys. Rev. A*, **32**, 506 (1985).
- Sahimi, M., B. D. Hughes, L. E. Scriven, and H. T. Davis, "Real-Space Renormalization and Effective Medium Approximation to the Percolation Conduction Problem," *Phys. Rev. B*, **28**, 307 (1983).
- Sahimi, M., G. R. Gavalas, and T. T. Tsotsis, "Statistical and Continuum Models of Fluid-Solid Reactions in Porous Media," *Chem. Eng. Sci.*, **45**, 1443 (1991).
- Sahimi, M., "Flow, Dispersion, and Displacement Processes in Porous Media and Fractured Rocks: From Continuum Models to Fractals, Percolation, Cellular Automata and Simulated Annealing," *Rev. Mod. Phys.*, **65**, 1393 (1993).
- Sahimi, M., "Nonlinear Transport Processes in Disordered Media," *AIChE J.*, **39**, 369 (1993).
- Seaton, N. A., and E. D. Glandt, "Percolation and Conduction in Colloidal Dispersions," *Physico Chem. Hydrodyn.*, **9**, 369 (1987).
- Stauffer, D., and A. Aharony, *Introduction to Percolation Theory*, 2nd ed., Taylor and Francis, London (1992).
- Stauffer, D., A. Coniglio, and M. Adam, "Gelation and Critical Phenomena," *Adv. Poly. Sci.*, **44**, 105 (1982).
- Stinchcombe, R. B., "Conductivity and Spin-Wave Stiffness in Disordered Systems; An Exactly Soluble Model," *J. Phys. C*, **7**, 179 (1974).
- Xu, J., and G. Stell, "An Analytic Treatment of Percolation in Simple Fluids," *J. Chem. Phys.*, **89**, 11101 (1989).
- Zemb, T. N., S. T. Hyde, P.-J. Derian, I. S. Barnes, and B. W. Ninham, "Microstructure from X-Ray Scattering: The Disordered Open Connected Model of Microemulsions," *J. Phys. Chem.*, **91** (1987).

Appendix

The interface separating the water and oil regions is constructed as follows: A random distribution of points in space is generated from the centers of a packing of hard spheres whose radius is adjusted to contain the water volume, counterions, and head groups as well as surfactant tails. Voronoi cells are constructed about each center so that their edges form a 3-D network. Adjacent points are then linked, forming a 3D random network that is the dual to the Voronoi tessellation. Since Voronoi cells for random hard-sphere packings have an average of 13.4 faces per cell, the random network has an average "coordination number" of links about each vertex Z of 13.4. To form a DOC cylinder model of coordination number Z , an average of Z of these links radiating from each vertex are sheathed with cylinders, and all network vertices are surrounded by spheres. This random network of cylinders and spheres represents an analytic approximation to a surface of constant average curvature, whose topology is characterized by the coordination number Z . The interfacial geometry so generated approximates the real surface of constant average curvature.

The ratio between the sphere and cylinder radii r_s/r_c is fixed by the requirement of equivalent packing of surfactant molecules in both regions. With the DDAB tails of length $\sim 10-15 \text{ \AA}$, $r_s/r_c \approx 2$ for sphere radii $r_s < 150 \text{ \AA}$ (which covers all values encountered in this study). For a fixed coordination number, the dimensions of the structure are then de-

termined completely, given the known surface area and internal volume fraction.

The interconnected water domains occupy a volume, ϕ_{int} , defined in the DOC structure with connectivity Z as

$$\phi_{\text{int}} = \left\{ \frac{4}{3} \pi r_s^3 - \frac{1}{3} Z r_c^3 \left[\Omega \rho^3 - \pi (\rho^2 - 1)^{1/2} \right] \right\} n + \left[\frac{8.15 n^{2/3} Z}{13.4} - (\rho^2 - 1)^{1/2} Z n r_c \right] \pi r_c^3 \quad (\text{A1})$$

where n is the density of sphere centers, ρ is the ratio of the sphere to cylinder radius, and Ω is the solid angle subtended by the cylinders where they intersect the spheres. The expression is derived from the total sphere volume, plus the cylinder volume between the spheres. The area occupied by the surfactant film is given by

$$\Sigma = (4 \pi r_s^2 - \Omega Z r_c^2) n + \left[\frac{8.15 n^{2/3} Z}{13.4} - (\rho^2 - 1)^{1/2} Z n r_c \right] 2 \pi r_c. \quad (\text{A2})$$

The surfactant head groups sit at this surface, the head-group area per surfactant molecule together with the composition setting the specific surface area. Since the model contains a surface that is strictly two-dimensional, the surfactant volume must be partitioned between the water and oil volumes. For the DDAB molecules, a head-group volume of $120 \text{ \AA}^3/\text{molecule}$ can be assigned to the water domains and a tail volume of $704 \text{ \AA}^3/\text{molecule}$ to the oil region (Zemb et al., 1987). The internal volume fraction of the structure (the water volume) is set by the specific volumes of the components and the composition. The preferred curvature of the surfactant is quantified by the surfactant parameter.

Equations A1 and A2 are solved numerically by stepping values of n , while Z and Σ are fixed to yield the prescribed values of ϕ_{int} . For a given Σ , ϕ_{int} , and Z the average and Gaussian curvatures can be calculated. The surfactant molecular shape, characterized by the surfactant packing parameter $(v/al)_{\text{eff}}$ is related to the average (H) and Gaussian (K) curvatures by:

$$\left(\frac{v}{al} \right)_{\text{eff}} = 1 + Hl + \frac{1}{3} Kl^2. \quad (\text{A3})$$

Equation A3 defines the effective molecular shape parameter for any ϕ_{int} , Σ , and Z . For a given value of ϕ_{int} and Σ , the coordination number Z may be adjusted to give the expected value of the surfactant packing parameter.

Manuscript received Jan. 18, 1994, and revision received May 23, 1994.